

Independent Component Analysis and Extended Kalman Filter for ECG signal filtering

1st Tasnim A. A. Mohammed
Electrical and Electronics Engineering)
Sakarya University
Sakarya, Turkey
tasnim.mohammed@ogr.sakarya.edu.tr

2nd Ayman E. O. Hassan
Electronics Engineering
University of Gezira
Wad Medani, Sudan
shatta@uofg.edu.sd

3rd Abdullah Ferikoglu
Electrical and Electronics Engineering
Sakarya University Of Applied Sciences
Sakarya, Turkey
af@subu.edu.tr

Abstract—During acquisition or transmission of the Electrocardiogram, noises generated from the surrounded electrical equipment, the patient's motion, movement of the electrodes, or contraction of the muscle around the heart usually interfere with the obtained signal. The interference of these noises in the frequency domain may mask the desired signal and obstruct the diagnosis process. Blind Source Separation techniques and Model-based filtering methods have shown promising results in ECG signal processing. This work pointed to assess the performance of Independent Component Analysis and Extended Kalman Filter in removing the most common ECG noise, such as muscle contraction, baseline shift, and electrode motion artifact. Testing has been executed on a formed signal set by adding noises from the MIT noise stress test database to signals from the MIT-BIH arrhythmia database at a different signal to noise ratio. Performance comparison demonstrates that both techniques show satisfying results in muscle artifact filtering, while ICA based filtration is more accurate than EKF in reducing baseline wander and electrode movement artifacts.

Index Terms—Electrocardiogram, Blind Source Separation, Model-based filtering, Independent Component Analysis, Extended Kalman filter, Signal to Noise Ratio

I. INTRODUCTION

The electrocardiogram (ECG) is a graph describes the action potential differences produced by depolarization and repolarization of the atria and ventricles measured on the body surface using electrodes. ECG signal shows the hearts rhythm, electrical conduction paths abnormalities, and chambers state. The clinicians use the electrocardiogram as an essential part of evaluating the human heart functions because of its relative ease of acquisition, analysis, and preciseness of information about heart abnormalities. The standard ECG signal consists of a series of repeated ECG cycle. Waves, segments, and intervals describe each cycle. The clinicians need to identify the cardiac cycle components for an accurate diagnosis.

ECG signal analysis stages are; signal preprocessing, noise filtration, detection of the cardiac cycle component, feature extraction, and formulation of the feature set [1]. The initial ECG analysis stage is noise and artifacts removal, which can have the same shape and within the frequency band of the ECG signal. ECG is susceptible to noise during the acquisition process due to muscle contraction, the patient's or electrode's

motion, and respiration. Also, the presence of devices around the patient represents another source of interference [2].

Filters detect, extract, or separate the desired signal from a noisy background and reduce noise components. Many of the available filtering techniques are based on the notion of spectral decomposition, such as using notch filters to reduce the power lines interference and bandpass filters to discard noise, which is localized in particular regions of the frequency spectrum. These techniques depend on the principle of linear superposition, and there is a fundamental assumption to reveal that the underlying signal and the noise are active in different parts of the frequency domain. The ECG signal frequency band is between 0.01-100 Hz. Signals with frequencies greater than 100 Hz or less than 0.01 Hz are considered as noise. Finite Impulse Response filters are used in all ECG devices to remove or reduce the undesired low and high-frequency noises. Low and high pass filters are implemented to cut out the high and low-frequency noise signals. Band-stop filters are selective filters used to remove the power line frequency, usually 50 or 60 Hz [3]. FIR filter's ability to reject noises and produce an ECG signal close as possible to the real heart potentials has been examined using several models. Mean square error (MSE) has been calculated for the response of different windowing techniques, FIR Chebyshev low pass filter has reduced the muscle artifact to the minimum [4]. The performance of various FIR and IIR filters has been computed and compared based on their SNR to ease the problem of selecting the appropriate filter order [5].

Filtering techniques are classified into linear and nonlinear. Wiener and Wavelet Filter are considered as linear filtering techniques applicable when both the signal and noise within the same region in the frequency domain, while model-based filtering and Blind Source Separation (BSS) are nonlinear techniques thus do not depend on the linearity constraints [2]. Many filters have been designed using Wiener and Wavelet Filters. An adaptive Wavelet Wiener Filter is proposed to remove myopotentials (EMG) noise and estimate a noise-free ECG signal [6]. The method achieved approximately 10.6 dB increment when tested on a generated database using signals from the CSE database, which is better than the traditional Wiener Wavelet-based Filtering methods. An improved Wavelet Wiener Filter has also been applied on CSE

database signals to overcome the linear filtering problem. SNR improvement (SNRI) for the introduced AWWF was 10.3 dB, while the SNRI for Wiener Wavelet Filter (WWF) was 5.2 dB [7].

Numerous researches were done in the area of ECG signal analysis and processing. However, recent advances in filtering, pattern recognition, and classification techniques have represented a new researching area in ECG signal analysis. Blind source separation techniques and model-based filtering methods show a positive impact on ECG signal processing. Over the past several years, source separation methods have gotten much consideration for their ability to separate noise sources from non-Gaussian noisy ECG signals and make them cleaner and better interpretable for clinicians. The ICA technique works on maximizing non-Gaussianity using higher-order statistics such as kurtosis and Negentropy. The maximization process is based on the central limit theorem [8].

ECG signal has a non-Gaussian shape; therefore, FASTICA has been employed to remove baseline wandering from a single channel ECG, which has been constructed to a multi-channel by adding some delay to the original signal. Results are derived by the proposed method were compared with those obtained from the traditional FIR high-pass filter [9]. Different ICA algorithms such as JADE and FASTICA have been studied and used for ECG denoising, with an effort to use constraint-ICA for noise separation [10]. FASTICA, with two granularity functions, hyperbolic tangent and power function, has been applied on randomly mixed data taken from the MIT-BIH arrhythmia database to isolate noise components from signal and noise mixture. Analysis of the obtained results demonstrated that tanh granularity function has quicker convergence when matched with the multi-granularity power function [11]. A Filter has been created based on the Kernel Principal Component Analysis (KPCA) algorithm to release the ECG signal from the effect of MA, EM, and BW noises. KPCA has given the lowest MSE compared to DWT and PCA based filtering and 5 dB SNR [12].

Model-based filtering techniques attempt to build a successful filter by finding an approximate signal or noise model. For ECG signals, extracting some features and then use them as parameters to develop a dynamical model can create a denoised signal. The first dynamical model for producing an artificial electrocardiogram has been introduced by (McSharry, 2003) [13]. The model consists of three joined conventional differential equations with the facility to specify the model parameters by the operator. The generated model has been fitted in real-time into ECGs collected from a healthy person, and another evaluation process has been done [14].

An effective filtering process using Extended Kalman Filter (EKF) has been performed on cardiac signals from MIT-BIH database. The previously presented nonlinear model has been linearized to apply the proposed EKF. Results clarify that the filter can successfully follow and remove noise components and produce better SNR [15], [16]. New filtering schemes have been built based on Extended Kalman Filter to train Multilayer Perceptron Neural Network [17]. The Wiener and Kalman

filter's ability to remove ECG signal noises has been measured using SNR, MSE, and Percentage RMS as evaluation metrics. Filtering gaussian, power line interference, muscle artifact, baseline wander, and composite noise using Wiener filter has produced average SNR higher than these achieved using Kalman filter [18]. Cubature Kalman filter (CKF) has been used to filter muscle artifacts and white Gaussian noises with input SNR from -5 to 10 dB. For white Gaussian noise, the output average SNR was about 11dB. In contrast, the CKF filter's output in the presence of muscle artifacts was 9 dB [19].

Here, the ICA's ability to eliminate muscle contraction, baseline shift, and electrode motion artifact has been investigated and compared with the performance of EKF in filtering the same noises.

II. THEORY

A. Independent component analysis (ICA)

ICA is a source separation method that transforms the data onto an independent set of vectors. ICA is a biorthogonal transformation project data mixture into non-orthogonal axes [14]. The following general mathematical framework is used to define ICA.

$$X = AS \quad (1)$$

X is the observed signals matrix, A is the mixing matrix, and S is the source signals matrix.

$$S = A^{-1}X = WX \quad (2)$$

W is a de-mixing matrix that is obtained by inverting the matrix A .

ICA assumes that the observed signals are linear mixtures of independent source signals to estimate the unknown source signals. The source estimation process can be achieved by non-linear decorrelation or maximizing the source non-gaussianity. The signal non-Gaussianity can be measured by maximum likelihood, mutual information, marginal entropy, Negentropy, and kurtosis [8].

Kurtosis is the normalized fourth-order cumulant. It is usually used to measure non-gaussianity for its computational and theoretical simplicity. When the data is preprocessed, its variance is equal to one $ES^2 = 1$. Kurtosis is given by:

$$kurt(s) = E[S^4] - 3(E[S^2])^2 \quad (3)$$

Various ICA algorithms have been developed, but FastICA and JADE algorithm are mostly used for ECG noise separation. RobustICA algorithm has been developed by (V. Zarzoso and P. Comon, 2010) as an improvement of FastICA. The algorithm achieves a precise line search of the absolute fourth-order moment to extract any nonzero independent component. In this method, the kurtosis divergence function is optimized globally at each de-mixing vector update to enhance the kurtosis in the search path [16].

RobustICA implements optimization at each iteration using an optimal step-size method; the process can be summarized as follow:

- 1) Set $i=0$ and give the de-mixing vector w an initial value.
- 2) Calculate the optimal step-size polynomial coefficients.
 $p(u) = \sum_{k=0}^4 a_k u^k$ The coefficients a_k can simply be acquired from the observed signal and the recent values of w and g .
- 3) Compute the fourth order polynomial roots $\{u_K\}_{k=1}^4$.
- 4) Choose the root which maximize the absolute value of fourth order moment within search path using:

$$u_{opt} = \max_k |kurt(w + u_k g)|$$

- 5) Update $w(i+1) = w + u_{opt} g$.
- 6) Normalize $w(i+1) = \frac{w(i+1)}{\|w(i+1)\|}$.
- 7) Calculate the estimated component value using $S_1 = wZ$.

While g is the search direction and typically the gradient $g = \nabla_w kurt(w)$.

$S = y_1, y_2, \dots, y_n$ are the estimated data matrix.

B. Extended Kalman Filter (EKF)

Kalman filter is a statistical method that optimally estimates past, present, and future states of an unknown variable within a set of noisy variables. The extended Kalman filter (EKF) is a modified version from the traditional Kalman that has been developed to work on the nonlinear dynamical models [2].

For a discrete nonlinear model and observation vector y_k , can be formulated as follows:

$$\begin{aligned} x_{k+1} &= f(x_k, w_k, k) \\ y_k &= g(x_k, v_k, k) \end{aligned} \quad (4)$$

Where f is the state space update function with state vector x_k , and w_k represents the process noise vector with associated covariance matrix $Q_k = E w_k \times w_k^T$. While g introduces the measurement function, which shows the relationship between the state vector and the observations, and v_k is measurement noise vector with associated covariance matrix $R_k = E v_k \times v_k^T$.

The above equation (4) need to be linearized around a specific point $(\hat{x}_k, \hat{w}_k, \hat{v}_k)$ in order to compute the Kalman Filter gain and the covariance matrix [20].

C. ECG Model and its Linearization

ECG is a series of repeated super quasi-periodic waves. The ECG model generator uses a series of exponentials to trace out the morphology of the ECG in the z -direction. The periodicity of the ECG makes the progress of the ECG track in a bounded cycle of unit radius. The extrema of the peaks (P, Q, R, S, T) is described by $(\theta_P, \theta_Q, \theta_R, \theta_S, \theta_T)$ in ECG generator. The following differential equations has been developed in [13] to represent ECG dynamical model equations, which are a set of three ordinary state in Cartesian coordinates.

$$\begin{cases} \dot{x} = \alpha x - \omega y \\ \dot{y} = \alpha x + \omega y \\ \dot{z} = -\sum_{i \in \{P, Q, R, S, T\}} a_i \Delta \theta_i \exp\left(-\frac{\Delta \theta_i^2}{2b_i^2}\right) - (z - z_0) \end{cases} \quad (5)$$

While $\alpha = 1 - \sqrt{x^2 + y^2}$, $\theta = a \tan 2(y, x)$ and $\Delta \theta_i = (\theta - \theta_i) \bmod(2\pi)$. Where x, y , and z are the state

variables, ω is the angular velocity of the track, θ is the four quadrant arctangent of the components of x and y , with $-\pi \leq \text{atan2}(y, x) \leq \pi$ and z_0 is the baseline. θ_i is the angular position for the PQRST waves, a_i is the magnitude of the peaks, b_i is the width (time duration) of each peak. Plotting z coordinate vs. time presents the artificial ECG signal [20].

The Cartesian form equations (5) can be rewritten in the polar form as follow:

$$\begin{cases} \dot{r} = r(1-r) \\ \dot{\theta} = \omega \\ \dot{z} = -\sum_{i \in \{P, Q, R, S, T\}} a_i \Delta \theta_i \exp\left(-\frac{\Delta \theta_i^2}{2b_i^2}\right) - (z - z_0) \end{cases} \quad (6)$$

The polar form is less complicated than the cartesian form. We can notice that r can be discarded since it does not affect the state variable z or any other variable.

The two-dimensional equations of the dynamic system can be simplified and written in the discrete form using a time step of size δt as follow:

$$\begin{cases} \theta_{k+1} = \theta(k) + \omega \delta t \\ z_{k+1} = -\sum_{i \in \{P, Q, R, S, T\}} \delta t a_i \Delta \theta_i \exp\left(-\frac{\Delta \theta_i^2}{2b_i^2}\right) + z(k) + \eta \delta t \end{cases} \quad (7)$$

Where $\theta(k)$ and $z(k)$ are the phase and ECG at time instant k , η is an additive noise that describes all the additive sources of process noise and replaces baseline wander, i is the number of Gaussian functions while θ_i represents the phase center of the i -th Gaussian.

In nonlinear dynamic models, the EKF is used to change the states over time but to complete the estimation process the model needs to be linearized to compute the Kalman filter coefficients. For this, θ and z are considered as the state variables and the model parameters $a_i, b_i, \theta_i, \omega, \eta$ are the process noises, By defining. In order to apply the EKF.

$$\begin{cases} x_{k+1} = F(\theta, \omega, k) \\ y_k = G(\theta, z, \omega, a_i, \theta_i, b_i, \eta, k) \end{cases} \quad (8)$$

The linearized model with respect to θ, z and process noise components is represented in [13]. The system process noise and covariance vectors are defined as follows:

$$\begin{cases} w_k = [a_P, \dots, a_T, b_P, \dots, b_T, \theta_P, \dots, \theta_T, \omega, \eta]^T \\ Q_K = E \{w_k w_k^T\} \end{cases} \quad (9)$$

The phase observations ϕ_k and the noisy ECG measurements s_k can be written in state space form as coming:

$$\begin{bmatrix} \phi_k \\ s_k \end{bmatrix} = \mathbf{I} \begin{bmatrix} \theta_k \\ z_k \end{bmatrix} + \begin{bmatrix} u_k \\ v_k \end{bmatrix} \quad (10)$$

Where $R_k = E[u_k, v_k]^T [u_k, v_k]$ is the observation noise covariance matrix.

III. METHOD

Despite the numerous research in the area of ECG signal processing, finding robust signal filtering techniques still form a challenge because the success of the noise reduction algorithm does not rely only on the nature of the signal but also depends on the noise nature.

A. ECG Filtering Using RobustICA

In this part, relying on the held comparison in [21] between newly proposed RobustICA and FastICA. RobustICA has been used for muscle artifact, baseline shift, and electrode motion noise separation from contaminated ECG signal using only two leads. Estimation method based on correlation has been performed to reconstruct a clean signal from the separated ICs. Signals are taken from the MIT-BIH database and mixed at a different ratio with noises taken from the MIT noise stress test database.

$$\begin{cases} \text{modified lead II} = \text{lead II} + N \\ \text{modified v5} = v5 + N \end{cases}$$

Where the modified leads represent the signal and noise mixture. Lead II and v5 are ECG signals taken from MIT-BIH database. N represents noise source (BW, MA, or EM) taken from MIT noise stress test database.

The steps of the algorithm can be described as follow:

- 1) Input: Observed noisy ECG signal.
- 2) Preprocessing: Subtract the signal mean, then Prewhiten the signal.
- 3) Estimate independent components using RobustICA.
- 4) Estimate mixing matrix H.
- 5) Calculate Kurtosis of estimated independent components..
- 6) Output: Estimated Filtered ECG signal.

B. ECG Filtering Using EKF

Extended Kalman Filter has been used for muscle contraction, baseline shift, and electrode motion artifact filtering from contaminated ECG signals. Using EKF formulation and the nonlinear state-space model presented in [22], estimation of the artifacts can be found. Process Equation:

$$\begin{cases} \theta_{k+1} = (\theta_k + \omega\delta) \text{mod}(2\pi) \\ s_{k+1} = -\sum_i^N \delta t a_i \Delta\theta_i \exp\left(-\frac{\Delta\theta_i^2}{2b_i^2}\right) + s_k + ? \end{cases} \quad (11)$$

δ is the sampling time, $\Delta\theta_i = (\theta_k - \theta_i) \text{mod}(2\pi)$, $\omega = 2\pi f$, f is heart rate, and N is the number of Gaussian functions.

$$\begin{cases} \phi_k = \theta_k + u_k \\ s_k = z_k + v_k \end{cases} \quad (12)$$

Where ϕ_k is the phase of the observations, and s_k is the measured noisy ECG. While u_k and v_k are the measurement noises.

The estimated de-noised ECG signal can be found from the following equation:

$$\hat{v}_k = y_k - \hat{s}_k \quad (13)$$

Where \hat{v}_k is the estimated de-noised ECG signal, y_k is the noisy ECG signal and \hat{s}_k is the estimated noise. The noise estimation process using EKF can be summarized as follow:

- 1) Input: measured noisy ECG signal.
- 2) Determine the location of R-peaks.
- 3) ECG phase calculation.
- 4) Mean ECG extraction.

- 5) Model fitting with the optimal parameter of mean ECG.
- 6) Apply EKF after calculating the covariance matrices of the measurement and process noise.
- 7) Output: subtract the noisy ECG signal y_k from the estimated noise signal \hat{v}_k to get the denoised signal \hat{s}_k .

IV. RESULT

The impact of the suggested methods has been studied on an artificial database that has been generated by selecting some ECG signals files from the MIT-BIH Arrhythmia database and mixing them with noise signals taken from MIT-BIH non-stress test database (NSTDB), which contains real ECG noises. The selected files have been segmented so that every Ten seconds represent a signal. The signals mixing process has been accomplished by adding the noise signal to the clean ECG signal to compose a noisy signal with the desired SNR. Seven combinations with different signal to noise ratio values extending from -20 to 20 dB have been generated for each segment. Then, the signal to noise ratio of the output signals has been calculated and compared with the input signal. The full testing has been simulated using MATLAB.

A. ECG noises removal using ICA

Baseline wandering (BW), Electrode motion (EM), and Muscle artifact (MA) signal has been combined with standard ECG signals to obtain noisy signals with a signal to noise ratio (20, 12, 6, 0, -6, -12, -20) dBs. These corrupted signals have been refined using RobustICA algorithm-based method. Table I contains the SNR before and after the filtering and percentage Mean Square Error values. Fig. 1, Fig. 2, and Fig. 3 show the noisy signal and the filtered signal. The blue line shows the noisy ECG signal and the red line displays the estimated noise-free signal.

TABLE I
SIGNAL TO NOISE RATIO VALUES AFTER USING ICA

SNR before filtering	After Filtering					
	Baseline wandering		Electrode motion		Muscle artifact	
	SNR	RMSE %	SNR	RMSE %	SNR	RMSE %
-20	-7.83	9.23	-6.54	9.32	-3.59	9.30
-12	0.17	8.83	-0.80	9.14	4.41	9.06
-6	6.17	8.48	7.46	8.81	10.41	8.68
0	12.17	8.28	13.46	8.47	16.41	8.26
6	18.17	8.17	19.46	8.26	22.41	7.98
12	24.17	7.99	25.46	8.09	28.41	7.60
20	32.17	7.63	33.46	7.59	36.41	7.54

From Table I using RobustICA with baseline wandering has increase SNR about 12 dB. Filtering the electrode movement artifact using RobustICA has improved the SNR of about 13 dB. While using RobustICA to remove the muscle artifact has raised the SNR of about 16 dB.

B. ECG noises removal using EKF

Noises have been mixed with ECG signal to obtain noisy signals with a signal to noise ratio (20, 12, 6, 0, -6, -12, -20) dBs. Table II contains noisy ECG signal SNR values and the

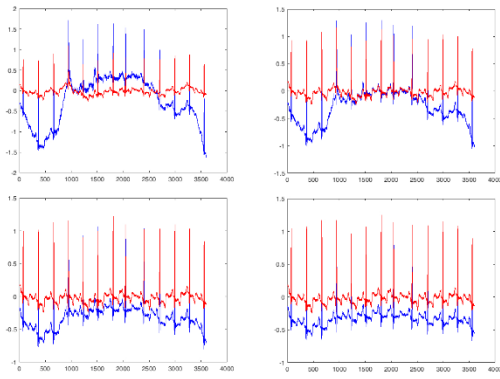


Fig. 1. Baseline wandering filtering.

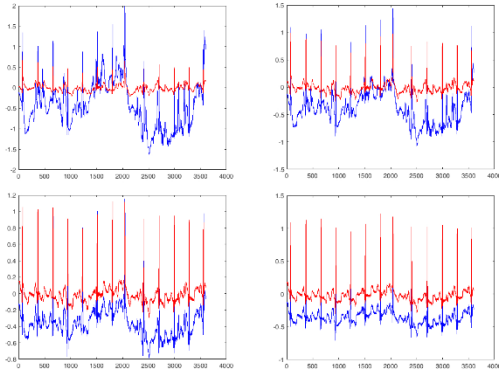


Fig. 2. Electrode motion artifact filtering.

estimated signals SNR values after using EKF, and the Model Error.

From Table II, signal to noise ratio improvement after using EKF in case of baseline wander reduction is about +2 dB, for electrode movement reduction is about +1.5 dB, and for muscle artifact removal is about +7 dB.

C. Comparison between ICA and EKF

From Fig. 4, SNR improvement after using RoboustICA to filter baseline wander is about +12 dB, while it is about +2

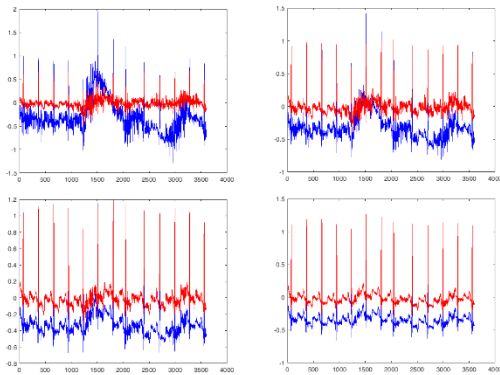


Fig. 3. Muscle artifact filtering.

TABLE II
SIGNAL TO NOISE RATIO VALUES AFTER USING EKF

SNR before filtering	After Filtering					
	Baseline wandering		Electrode motion		Muscle artifact	
	SNR	ME	SNR	ME	SNR	ME
-20	-17.91	0.07	-18.57	0.18	-12.72	0.94
-12	-9.91	0.09	-10.91	0.10	-4.74	0.58
-6	-3.98	0.25	-4.93	0.12	1.05	0.26
0	1.96	0.19	1.41	0.19	7.44	0.24
6	7.22	0.11	7.78	0.16	13.16	0.14
12	11.45	0.38	13.04	0.14	18.14	0.15
20	21.81	0.14	18.41	0.13	20.71	0.14

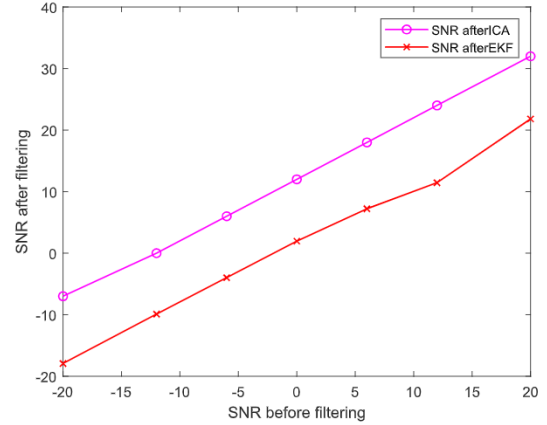


Fig. 4. Baseline wandering removing using ICA and EKF.

dB after using EKF.

From Fig. 5, SNR enhancement after using RoboustICA to remove electrode movement artifact is about +13.5 dB, while SNR improvement after using EKF is about +1.5 dB.

From Fig. 6, SNR change after using RoboustICA to filter muscle artifact is about +16.5 dB, while SNR advance after using EKF is about +7 dB.

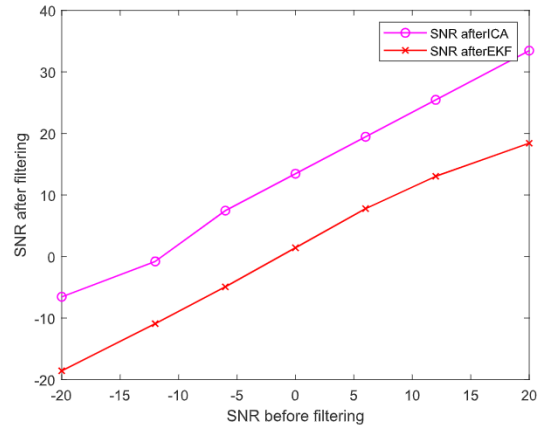


Fig. 5. Electrode motion artifact removing using ICA and EKF.

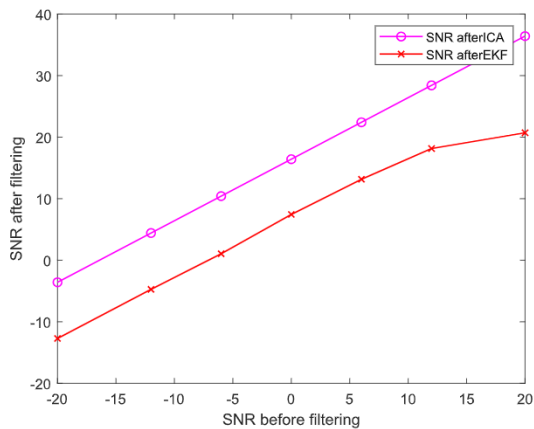


Fig. 6. Muscle artifact removal using ICA and EKF.

V. DISCUSSION AND CONCLUSIONS

This work has been concerned with studying the ECG signal and the noises that mask it to develop an efficient and reliable algorithm to reduce muscle contraction artifact, baseline shifting, and electrode motion noises as the most common ECG noises. Two algorithms have been applied; Independent Component Analysis (RobustICA), which separates the contaminated observed signal into independent components, and model-based filtering using Extended Kalman Filter (EKF).

To assess the success of the suggested method, an artificially produced database has been built by mixing noise-free ECG signals with baseline wander, muscle artifact, and electrode movement noises to create signals with Signal to Noise Ratio (SNR) 20, 12, 6, 0, -6, -12, and -20 dB.

The results of the analysis demonstrate that RobustICA gives better results in the decline of muscle artifact when matched with the reduction ratio of baseline wander and electrode movement artifacts. Simultaneously, EKF shows promising results in decreasing muscle artifact when the signals have low SNR. The analysis results also demonstrate that RobustICA is more beneficial than EKF in decreasing baseline wander and electrode movement artifacts while both show promising results in reducing muscle artifact. RobustICA based estimation algorithm performed better than the EKF method by producing better SNR in the presence of all common types of artifacts.

REFERENCES

- [1] U. R. Acharya, S. M. Krishnan, J. A. Spaan, and J. S. Suri, *Advances in cardiac signal processing*. Springer, 2007.
- [2] G. D. Clifford, F. Azuaje, P. McSharry *et al.*, *Advanced methods and tools for ECG data analysis*. Artech house Boston, 2006.
- [3] H. Limaye and V. Deshmukh, "Ecg noise sources and various noise removal techniques: a survey," *International Journal of Application or Innovation in Engineering & Management*, vol. 5, no. 2, pp. 86–92, 2016.
- [4] M. T. Almalchy, V. Ciobanu, and N. Popescu, "Noise removal from ecg signal based on filtering techniques," in *2019 22nd International Conference on Control Systems and Computer Science (CSCS)*. IEEE, 2019, pp. 176–181.

- [5] N. Das and M. Chakraborty, "Performance analysis of fir and iir filters for ecg signal denoising based on snr," in *2017 Third International Conference on Research in Computational Intelligence and Communication Networks (ICRCICN)*. IEEE, 2017, pp. 90–97.
- [6] L. Smital, M. Vitek, J. Kozumplik, and I. Provaznik, "Adaptive wavelet wiener filtering of ecg signals," *IEEE transactions on biomedical engineering*, vol. 60, no. 2, pp. 437–445, 2012.
- [7] R. Chandu and M. Venkateswarlu, "Ecg signal filtering using an improved wavelet wiener filtering," *International Journal of Advanced Technology and Innovative Research*, vol. 7, no. 7, pp. 1242–1247, 2015.
- [8] A. Hyvärinen and E. Oja, "Independent component analysis: algorithms and applications," *Neural networks*, vol. 13, no. 4-5, pp. 411–430, 2000.
- [9] Z. Barati and A. Ayatollahi, "Baseline wandering removal by using independent component analysis to single-channel ecg data," in *2006 International Conference on Biomedical and Pharmaceutical Engineering*. IEEE, 2006, pp. 152–156.
- [10] A. S. Barhatte, R. Ghongade, and S. V. Tekale, "Noise analysis of ecg signal using fast ica," in *2016 Conference on Advances in Signal Processing (CASP)*. IEEE, 2016, pp. 118–122.
- [11] M. Phegade, P. Mukherji, and U. Sutar, "Hybrid ica algorithm for ecg analysis," in *2012 12th International Conference on Hybrid Intelligent Systems (HIS)*. IEEE, 2012, pp. 478–483.
- [12] M. M. V. Gualsaquí, E. I. P. Vizcaíno, M. J. Flores-Calero, and E. V. Carrera, "Ecg signal denoising through kernel principal components," in *2017 IEEE XXIV International Conference on Electronics, Electrical Engineering and Computing (INTERCON)*. IEEE, 2017, pp. 1–4.
- [13] P. E. McSharry, G. D. Clifford, L. Tarassenko, and L. A. Smith, "A dynamical model for generating synthetic electrocardiogram signals," *IEEE transactions on biomedical engineering*, vol. 50, no. 3, pp. 289–294, 2003.
- [14] R. Sameni, M. B. Shamsollahi, C. Jutten, and M. Babaie-Zade, "Filtering noisy ecg signals using the extended kalman filter based on a modified dynamic ecg model," in *Computers in Cardiology, 2005*. IEEE, 2005, pp. 1017–1020.
- [15] O. Sayadi and M. B. Shamsollahi, "Ecg denoising and compression using a modified extended kalman filter structure," *IEEE Transactions on Biomedical Engineering*, vol. 55, no. 9, p. 2240, 2008.
- [16] O. Sayadi, R. Sameni, and M. B. Shamsollahi, "Ecg denoising using parameters of ecg dynamical model as the states of an extended kalman filter," in *2007 29th Annual International Conference of the IEEE Engineering in Medicine and Biology Society*. IEEE, 2007, pp. 2548–2551.
- [17] S. Gaamouri, M. B. Salah, and R. Hamdi, "Denoising ecg signals by using extended kalman filter to train multi-layer perceptron neural network," *Automatic Control and Computer Sciences*, vol. 52, no. 6, pp. 528–538, 2018.
- [18] B. Manju and M. Sneha, "Ecg denoising using wiener filter and kalman filter," *Procedia Computer Science*, vol. 171, pp. 273–281, 2020.
- [19] R. M. Bodile and T. H. Rao, "Ecg denoising using cubature kalman filter framework," in *2020 5th International Conference on Communication and Electronics Systems (ICES)*. IEEE, 2020, pp. 228–232.
- [20] R. Sameni, M. Shamsollahi, and C. Jutten, "Filtering electrocardiogram signals using the extended kalman filter," in *2005 IEEE Engineering in Medicine and Biology 27th Annual Conference*. IEEE, 2006, pp. 5639–5642.
- [21] V. Zarzoso and P. Comon, "Robust independent component analysis by iterative maximization of the kurtosis contrast with algebraic optimal step size," *IEEE Transactions on neural networks*, vol. 21, no. 2, pp. 248–261, 2009.
- [22] M. S. Grewal and J. Kain, "Kalman filter implementation with improved numerical properties," *IEEE transactions on automatic control*, vol. 55, no. 9, pp. 2058–2068, 2010.